Urban climate influence on building energy use

K. R. Gunawardena and T. Kershaw

Department of Architecture and Civil Engineering, University of Bath,
Claverton Down, Bath, BA2 7AY, UK.
Corresponding author: T. Kershaw, t.j.kershaw@bath.ac.uk

Abstract

Building energy demand in cities is expected to be affected as a warming climate, increasing frequency and severity of extreme heat events, and the urban heat island effect (UHI) cumulatively exacerbate heat related risks. To mitigate such climate loading and reduce energy bills, the way that buildings are constructed have changed over recent decades. This paper examines not only how the UHI affects space-conditioning loads within urban office buildings, but also how the trend of replacing traditional heavyweight stone facades with lightweight highly glazed and insulated ones affects both the magnitude and timing of the UHI and resulting building energy use. The paper addresses this through a simulation study of a typical street canyon based on the Moorgate area of London. Results show that including the UHI within a dynamic thermal simulation has an adverse effect on annual space-conditioning, with a 4 % increase in demand for buildings with stone facades, while those with a glazed construction show a 10 % increase. The study therefore demonstrates that the trend in urban centres to construct highly glazed buildings with lightweight insulated facades increases space-conditioning loads and consequently adversely affects the UHI, thereby creating a vicious cycle of additional urban heating that exacerbates the impacts of climate change. The study in turn stresses the significance of accounting for UHI loads in estimating urban energy use, for which a combined simulation approach has been presented as a practical pathway.

1 Introduction

Projections of climate change and increasing frequency and severity of extreme heat events are likely to have an adverse influence on the global trend towards urbanisation (UN 2014). In addition to such global and synoptic scale climate modifications, the meso-to-microscale urban setting is challenged by the long-established warming induced by the heat island effect (UHI) (Howard 1833, Oke 1987). Collectively, such global-to-microscale climatic conditions exert significant influence on the sustainable operation of urban settlements. Understanding the interactions between the built-environment and its dynamic climatic context is therefore necessary for the sustainable planning of urban growth.

$$\text{Net radiation} + \text{Anthropogenic heat} = \text{Convection} + \text{Evaporation} + \text{Heat storage} \quad (1)$$

Essential to this understanding is the ‘urban energy balance’ Eq. (1), which represents the partitioning of incoming and outgoing energy flows of the urban surface system (Oke 1982). The typically warmer climate experienced in such urban areas is explained by the net positive thermal balance that leads to the formation of UHIs. This net positive thermal balance arises from changes to their surface properties such as increased surface roughness, reduced albedo, reduced green and blue space for evaporation, and increased heat generated from human activities (anthropogenic heat). The resulting UHI effect can be considered as an added environmental thermal load that affects how energy is used within buildings (Grimmond et al. 2010). This energy use is also a contributing heat source of the UHI. Higher building energy usage could therefore contribute to the storage of greater thermal energy in the urban system and thereby help generate and intensify UHIs (Oke 1987). This suggests that if high-energy solutions are used to ventilate and cool buildings, a vicious cycle of warming may result, creating an ever worsening and unhealthy urban environment. This is made more complicated by the regeneration of inner-city areas following a trend of replacing traditional modestly glazed heavyweight façades with lightweight highly

glazed and insulated ones. The purpose of this study is to identify this influence and its degree of significance to building energy loads through the comparison of 'dense and opaque', and 'light and transparent' dominant construction build-ups. The method for addressing this considers simulations of an idealised central canyon, based on the morphology of the Moorgate area of London (Figure 1b).

1.1 Applied model: the Urban Weather Generator

To overcome the many challenges of accounting for the complexities of the interconnected urban climate, this study uses a modified version (5.1.0 beta, Norford et al. 2017) of the multiscale coupled framework termed the 'Urban Weather Generator' (UWG) (Norford et al. 2015). The UWG presented schematically in Figure 1a, is based on Monin-Obukhov similarity theory and is composed of four coupled sub-models that include a Rural Station Model (RSM), Vertical Diffusion Model (VDM), Urban Boundary Layer Model (UBLM), and an Urban Canopy and Building Energy Model (UC-BEM) based on the Masson (2000) Town Energy Balance scheme and a building energy model developed by Bueno et al. (2012). These sub-models exchange data to calculate modified temperature and humidity values and compile a modified weather file in the EnergyPlus (.epw) format for use by dynamic building thermal modelling software. A summary of the basic data exchanges involved is presented in Figure 1a, while detailed descriptions are offered in Bueno et al. (2013), (2014). The UWG has been verified against field data from Basel, Toulouse, and Singapore (Bueno et al. 2013, 2014, Nakano et al. 2015). The verifications from Basel and Toulouse demonstrated that urban climate estimation requires both canopy and boundary layer effects in order to account for the aggregated influence of the UHI over the entire city; with more than half the influence observed in urban canyons attributed to the mesoscale effect. The resolution of such boundary layer influences require mesoscale processes to be reconciled with the aid of higher-scale atmospheric simulations coupled within a framework as employed by the UWG (Bueno et al. 2013).

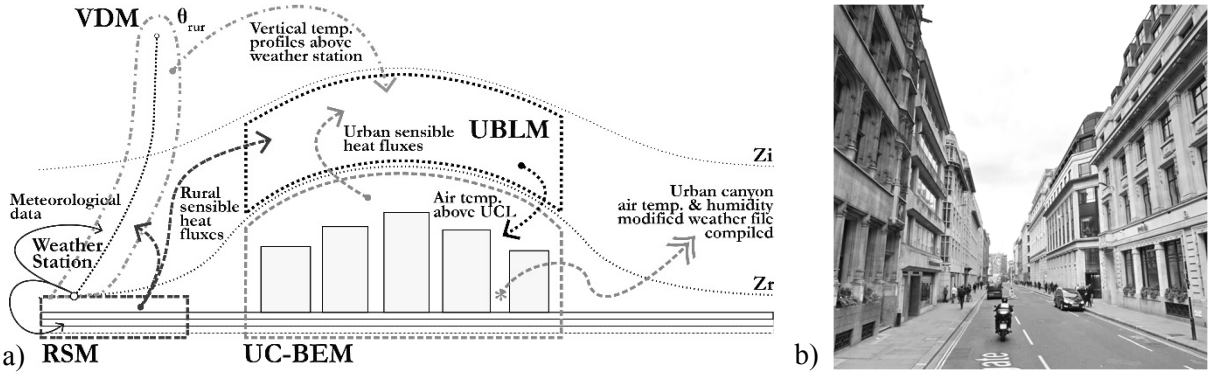

Figure 1. Domain of the UWG modules and data exchanges in an ideal city, based on Bueno et al. (2013) (a); Typical street canyon view of Moorgate, London, from ©Google Street-view, 2017 (b).

2 Method

The morphology of the Moorgate area in London is idealised in this study by averaging parameters to produce an urban roughness profile with a characteristic radius of 500 m. The characteristics of this urban roughness (detailed in Appendix: Table 2), together with a rural weather file (in .epw format) are input into the UWG (5.1.0 beta) to generate weather profiles that account for the UHI influence on air temperature and humidity values for the canyon scenarios considered (see Table 1). The rural weather data used for this study is the Design Summer Year (DSY) for the Reading area (60 km due west of the Moorgate site), which was generated using the UKCP09 Weather Generator, the full methodology of which is described in Eames et al. (2011).

The generated UWG profiles for the canyon scenarios were then applied to a thermal model of the Moorgate street canyon and surrounding buildings, created in the dynamic simulation modelling package IES-VE (2015) to estimate space-conditioning loads for the respective scenarios.

Table 1. Simulation scenarios.

Scenario	Weather file used	Construction
Base Stone	Design Summer Year (DSY) for Reading (unmodified).	Using stone facades with a glazing ratio (GR) of 0.30, detailed in Appendix: Table 2 (currently dominant among buildings of Moorgate).
Stone: 0.30	The above modified using the UWG, i.e. with the dominant construction of Stone facades and resulting UHI influence included.	
Base Glazed	Design Summer Year (DSY) for Reading (unmodified).	Using glazed facades with default GR: 0.30, detailed in Appendix: Table 2 (hypothetical scenario).
Glazed: 0.30	The above modified using the UWG, i.e. with the dominant construction of Glazed facades and resulting UHI influence included.	Additional hypothetical variations using the following GRs: Glazed A: 0.15; Glazed B: 0.30; Glazed C: 0.50 and Glazed D: 0.90.

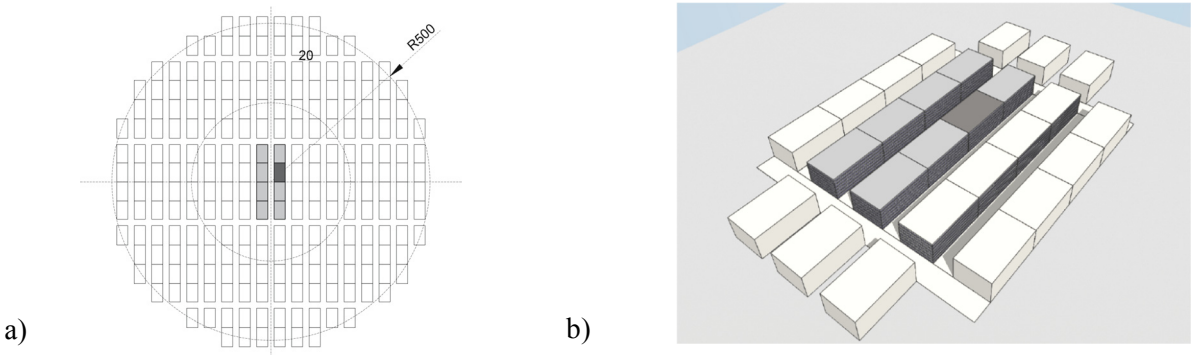

Figure 2. Idealised 500 m radial urban configuration based on Moorgate morphology used for UWG climate file generation (a); focused area of the street canyon considered for IES-VE energy simulations (b).

3 Results

The following considers firstly, the features of the urban weather files generated by the UWG with the influence of the UHI included, and secondly, their cooling and heating load implications for the highlighted building in Figure 2a, b that belongs to the central Moorgate street canyon.

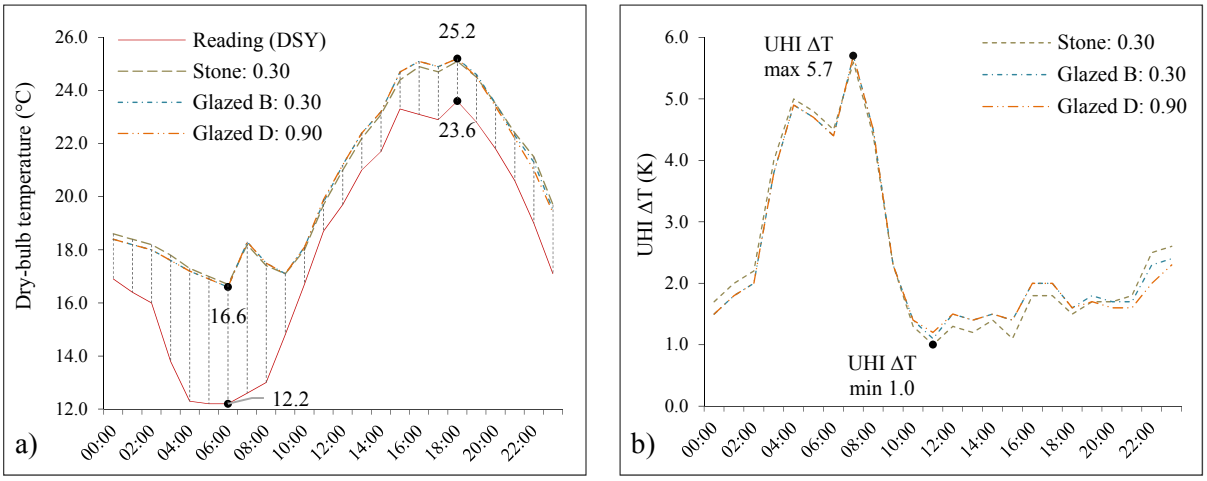

Figure 3. Summer solstice (21-Jun) dry-bulb temperature profiles (a); and UHI ΔT or intensity profiles (K) (b); for Stone, Glazed B, and Glazed D scenarios relative to the Base Reading (DSY) profile.

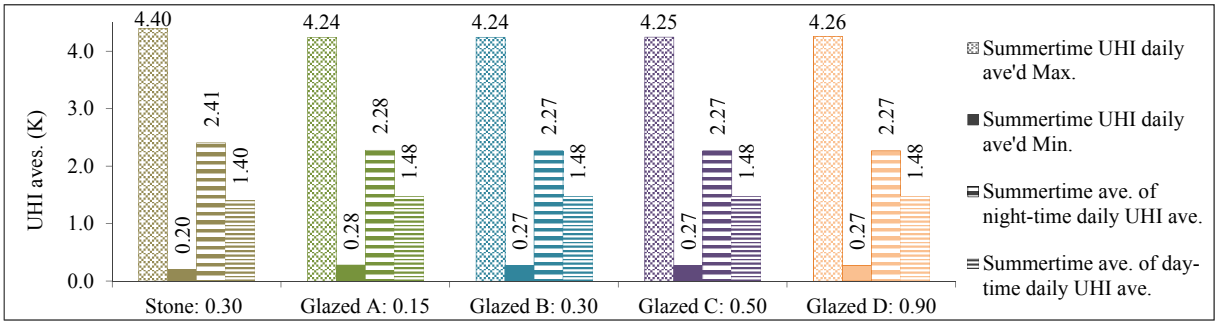

Figure 4. Summertime (May-Sep) UHI features for scenarios simulated (K).

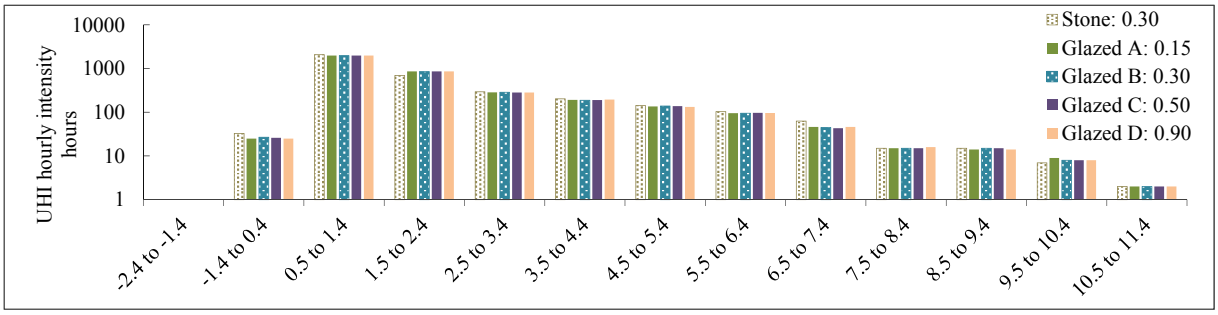

Figure 5. Summertime (May-Sep) UHI intensity (K) frequencies, Log10 (hours).

3.1 Canyon microclimate profiles

The summertime UHI average daily maximums for these scenarios range from 4.24 to 4.40 K, while the average daily minimums range from 0.20 to 0.27 K (Figure 4). Although the latter average daily minimums are positive values, hourly UHI intensity or ΔT data identified cool islands (negative ΔT) in all scenarios with intensities ranging from <0 to -2 K that represented ~1.7 - 2.5 % of the (3,672) hours simulated. These hourly UHI ΔT values also identified peaks ranging from >6.4 to ≤12.4 K that represented 2 - 3 % of the total hours simulated (Figure 5). Notably, the Stone scenario showed the highest hours reaching peak and minimum values (max ~3 %, min ~2.5%) relative to Glazed scenarios.

When hours of the day are separated into daytime (from 6 AM to 6 PM) and night-time (the residual) UHI intensity values, the daily daytime averages ranged from 1.39 to 1.48 K, and night-time averages ranged from 2.27 to 2.41 K. The night-time averages therefore were higher than daytime values. While this is true for averages, the summer solstice (21-June) illustrates an example where the hourly UHI ΔT maximum for the day was reached in the morning at around 7 AM, almost two hours after sunrise (around 4:50 AM) (Figure 3b). This summer solstice UHI profile also showed that the night-time averages were higher for the Stone scenario relative to Glazed scenarios, while the converse was true during the midday to evening period of the day.

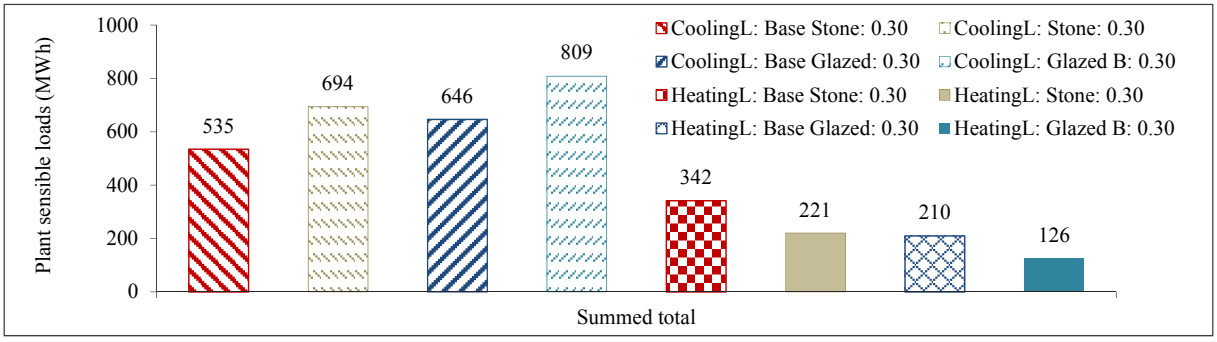

Figure 6. Cooling and heating plant sensible loads for Base and including UHI influence for both Stone and Glazed facade simulations (all with GR: 0.30).

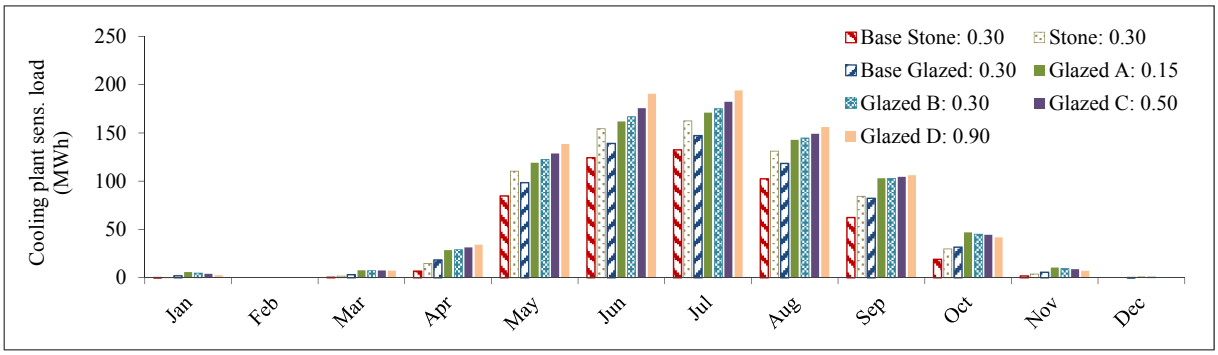

Figure 7. Cooling plant sensible load monthly totals (MWh).

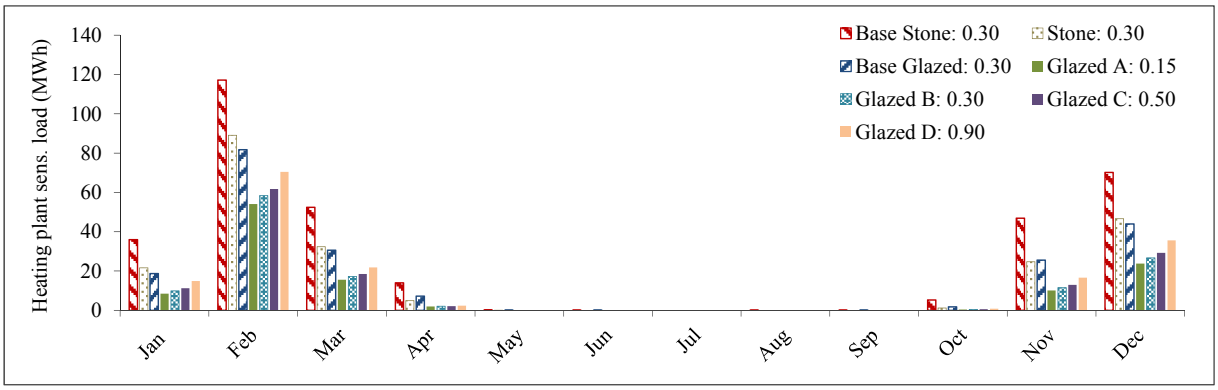

Figure 8. Heating plant sensible load monthly totals (MWh).

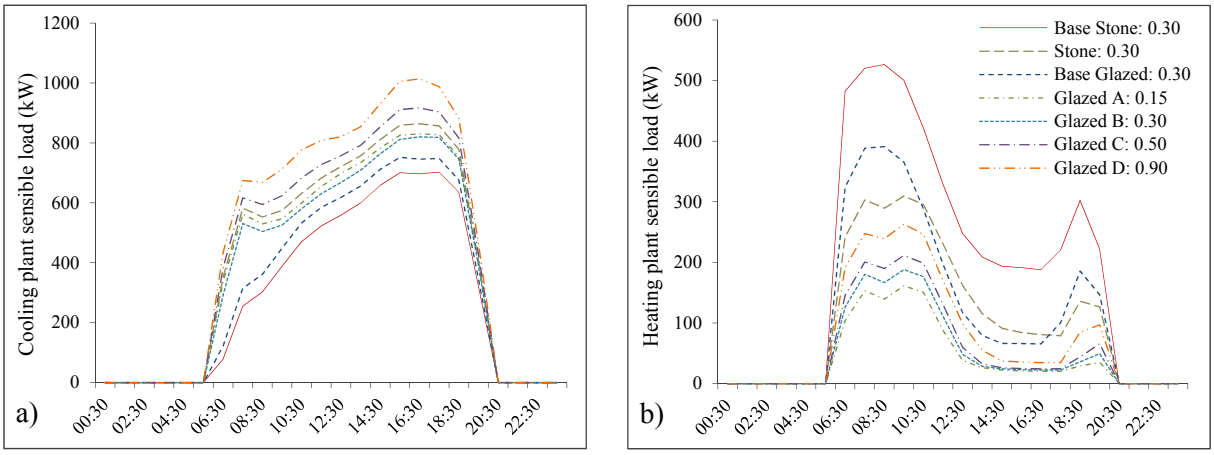

Figure 9. Summer solstice (21-Jun) cooling load (a); winter solstice (21-Dec) heating load (b); (kW).

3.2 Space-conditioning loads

Including UHI influence on heating and cooling load values (Figure 6 to Figure 9) demonstrated significant differences between the Stone and Glazed scenarios. For the Stone scenario relative to its Base Stone simulation, including the UHI influence resulted in a 30 % increase in summertime cooling demand, while winter heating demand was reduced by 36 %. Overall, this meant that the influence of the UHI had an adverse effect on the space-conditioning demand of around 37 MWh, or a 4 % increased demand for the office building (Figure 6). When the Base Glazed scenario was compared against the Glazed scenario B simulation that included the UHI influence (both with GR: 0.30), this resulted in a 26 % increase in cooling demand and a 41 % decrease in heating demand. Overall, this meant that the influence of the UHI had an adverse effect on the space-conditioning demand of around 82 MWh or a 10 % increased demand for the office building (Figure 6).

When Glazed scenarios A to D were considered (Figure 7 and Figure 9a), cooling demands showed considerable increase relative to the Base Glazed simulation, with scenario D showing the greatest (36 %), and scenario A with the lowest (24 %) increase. In contrast when heating loads were considered, scenarios A through to D showed reduced demands with scenario A showing the greatest (46 %), and scenario D with the lowest (22 %) decrease (Figure 8 and Figure 9b). The effect of GR increase addressed by the relative comparison to Glazed A scenario with the lowest GR: 0.15, showed net space-conditioning demand increase respectively to D scenario with GR: 0.90 (B=40, C=106, D=227 %, increases relative to A). The effect of transforming the heavyweight facades to lightweight glazing addressed by the comparison between the Stone scenario against Glazed B scenario (both with GR: 0.30 and UHI influence included), showed the net effect on annual space-conditioning load demand increased by around 21 MWh or a 2.3 % increase for the office building (relative heating load reduced by 43 %, although cooling load increased by 17%, see Figure 6).

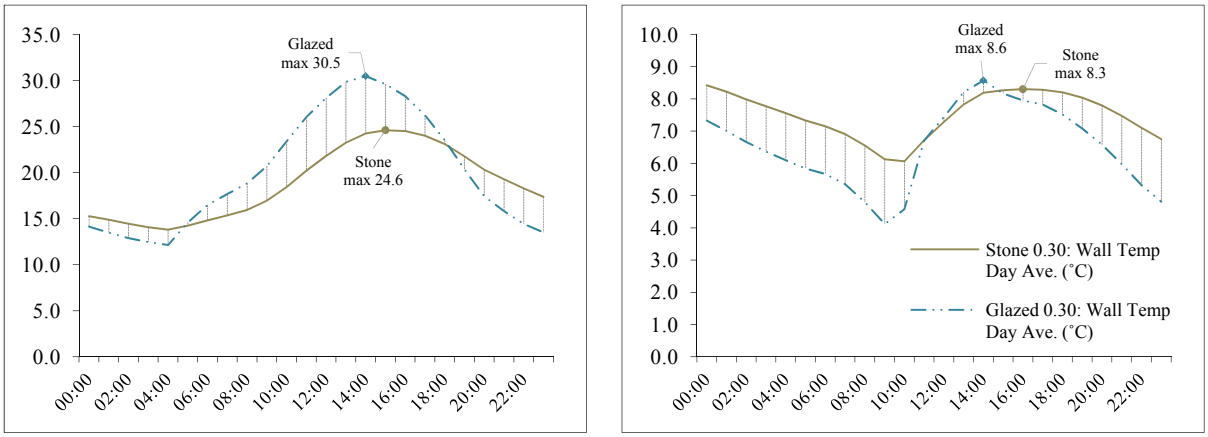

Figure 10. Summer solstice (21-Jun) (a); winter solstice (21-Dec) (b); building wall surface temperatures (˚C).

4 Discussion

Historical observations of the London UHI reveals a diverse representation. The earliest observations of Howard (1833) noted that London was 0.6 K warmer in July, while in November was 1.2 K warmer than the country. Howard (1833) also observed that at night it was 2.05 K warmer, and during the day 0.19 K cooler relative to the country. Examining temperature data for the period from 1931-60, Chandler (1965) found the annual mean to be 1.4 K warmer for central London, and noted 0.9 K warmer daytime maximum temperatures, with summertime monthly mean value of 1.6 K, and 1.2 K for winter. More recently, Watkins et al. (2002) presented measured data from 1999 to show a summertime (Jun-Aug) excess of ~2.8 K, and a peak value of 8 K. Data from 1999 also demonstrated a maximum summertime daytime UHI of 8.9 K, while a maximum nocturnal UHI of 8.6 K was found during clear-sky periods when the wind velocity was below 5 ms^{-1} (Kolokotroni and Giridharan 2008). In winter their data showed that the maximum UHI was 9 K both day and night with similar wind velocities (Giridharan and Kolokotroni 2009). In a recent study of west London urban parks, Doick et al. (2014) observed summertime nocturnal UHI peaks of 10 K on certain nights.

In this study the summertime average UHI for the street canyon ranged between 1.84 to 1.86 K for the scenarios simulated. Considering the above historic values and the results presented earlier, the UHIs simulated by the UWG could be said to fall within a plausible range. The lower UHI averages for the daytime relative to the night-time simulated across the scenarios is consistent with most UHI studies (Oke 1987, Wilby 2003). However, Howard's (1833) finding of 0.19 K cooler daytime (i.e. cool island) London temperatures relative to the country was not predicted by any of the simulations of this study. In general, the occurrence of cool island conditions were noticeably less than expected at this canyon and were limited to hourly occurrences as noted in the results section. This may be attributed in this study to the 20 m street width being wide enough to minimise the canyon shading effect, and the notably

higher anthropogenic heat output used for the Moorgate area (based on data from the Iamarino et al. (2012) simulation study) contributing to relatively higher daytime canyon temperatures. This latter significance of anthropogenic heat output is demonstrated by the summer solstice UHI profile (Figure 3a, b). With this profile, although the night-time UHI had accumulated heat to present reasonably higher canyon temperatures around dawn (~4-5 AM), the onset of the office building activity profile provides a boost of anthropogenic heat to elevate (spike) temperatures to reach an even higher UHI ΔT maximum at a delayed peak time after 7 AM.

When the summertime average UHI for the canyon and its breakdown into daytime and night-time averages were considered, the Stone scenario presented higher values relative to Glazed scenarios. When hourly resolution data was reviewed, the Stone scenario showed the highest proportion of hours reaching UHI ΔT maximum values. This suggests that urban fabrics with dominant heavyweight stone constructions such as at Moorgate could generate a warmer heat island effect to be experienced in the street canyon particularly at night, relative to ones dominated by lightweight glazed constructions. The Stone scenario also showed the highest proportion of hours reaching UHI ΔT minimum values, predominantly during the day. This indicates that even though this material profile has the potential to generate a warmer canyon temperature profile in the night-time, during the daytime it also has the potential to contribute greater to the experience of cool island conditions. This observation may be attributed to the buffering properties offered by the thermal mass of heavyweight materials such as stone.

The materiality of urban form influences the surface energy balance by affecting both net radiation and heat storage. The radiative properties of materials are considered as emissivity and albedo, while storage properties are affected by heat capacity and thermal conductivity. The radiative property of albedo (α) or solar reflectance is defined as the percentage of solar energy reflected by a surface, and is a significant determinant of material surface temperatures (Oke 1987, Taha 1997, Jacobson 2005). Since 43 % of solar energy is in the visible wavelengths (400-700 nm), material colour is strongly correlated with albedo, with lighter coloured surfaces having higher values (α ~0.7) than darker surfaces (α ~0.2) (Taha et al. 1988). In this study the stone is assumed to be Portland (typical for the Moorgate area), which is of a lighter colour and a relatively high mean albedo of 0.6. This in turn contributes to lower radiation absorption by the facade material that helps to reduce its surface temperature. As Figure 10a, b for summer and winter solstice surface temperature profiles for external walls demonstrate, during the midday period the temperature is lower for Stone surfaces compared to Glazed. Furthermore the difference is more pronounced during the summer when solar radiation contribution is at its greatest. This surface temperature difference between heavyweight and lightweight constructions can affect the urban microclimate both directly and indirectly. The direct effect is experienced in the form of its influence on reducing canyon ambient temperatures as relatively cooler surfaces would have relatively lower sensible flux. The indirect effect works in conjunction with material heat storage properties to modify building energy use and its feedback to the microclimate.

Higher degrees of radiation reflection from high albedo materials mean that less energy is available for transfer into their depth. From the residual energy that is absorbed, a material's ability to store heat (capacity), which at times is referred to as thermal mass, and thermal diffusivity, the ease by which heat penetrates into a material (function of thermal conductivity and volumetric heat capacity), determines its thermal inertia, a measure of the responsiveness of a material to temperature variations. Heavyweight materials such as stone have relatively higher diffusivity, heat capacity, and thermal inertia, which means that their temperature fluctuations through the diurnal cycle are minimised (Gartland 2008). Thus, when radiation energy is received by such surfaces, the non-reflected energy is mostly absorbed and stored and when the climate above is relatively cooler, is re-radiated (as longwave) or purged back to the climate. This lag is evident when examining both surface temperature profiles (Figure 10), which show a lower daily variability range (amplitude) and delay in peak (phase shift) for Stone surfaces relative to Glazed surfaces. From the building's perspective, the material of the envelop absorbing more heat and storing it means that less thermal energy is making its way into the internal environments. This in turn helps to reduce their cooling loads and resulting heat rejection feedback to the climate, which is

particularly evident in the daytime. This storage benefit of the heavyweight stone facade however can have a negative effect in the winter, as a significant proportion of the initial energy expenditure may be used to heat the facade rather than the internal environment. Lightweight glazed constructions on the other hand demonstrate faster response to microclimate thermal changes, which explains the reduced demand in winter heating load (Figure 8). Including the higher thermal load from the UHI therefore transfers readily into the internal spaces of the building to present a significant 'winter warming effect' (40 % reduction with the same GR: 0.30). However, increasing the areas of glazed fabric area (GR) predictably increases fabric heat loss, which in turn reduces the winter warming effect experienced. In the summer, it is clear that the higher cooling demand in such scenarios is generated by the increased solar gain that results with increased glazed facade areas.

Materiality of urban built form can influence both the properties of the UHI as well as its impact on the building performance of this built form. The properties of the dominant material profile in an urban setting is identified in previous research to modify the intensity and timing of when the UHI peak is likely to be observed (Oke 1987). Cities made of predominantly lower diffusivity materials are therefore suggested to reach their UHI peak soon after sunset, while those made with higher diffusivity materials such as stone are unlikely to reach theirs until sunrise (Gartland 2008). This study demonstrates this to be true for the Stone scenario with the peak evident towards sunrise. However, the Glazed scenarios do not demonstrate the phase shift to confirm the suggested observation for lightweight constructions (Figure 3a, b). Conversely, the thermal efficiencies of the building envelope have a significant influence on the degree of benefit or detriment to their space-conditioning loads presented by the UHI load. In this study, the space-conditioning loads demonstrated that a Stone construction could be said to accommodate the additional thermal load from the UHI relatively better over the course of the year than a lightweight Glazed construction of the same GR.

5 Summary

In an urban development, the material constructions used and their properties of emissivity and albedo, together with heat capacity and thermal conductivity, determine how solar energy is reflected, emitted, and absorbed by surfaces. The properties of the dominant material within this urban setting may affect the intensity and the timing of when the UHI peak is likely to be observed, and how the UHI load itself is transferred into internal environments, thereby affecting their space-conditioning performance. However, the selection of materials for constructing urban developments is influenced by many other factors in addition to their thermal properties. Buildability and assembly issues, economics, supply, regulatory guidance, cultural and historic context, and aesthetics can all influence the materiality of a development or even the character of entire cities subject to which influence gains primacy. It is worth noting that materiality is an aspect of existing built-environments that can be reasonably altered to offer heat mitigation, perhaps to a greater degree of practicability than the alteration of existing morphology.

The study has shown that the trend in urban centres to construct highly glazed buildings with lightweight insulated facades increases space-conditioning loads and adversely affects the UHI, thereby creating a vicious cycle of additional urban heating that exacerbates the impacts of climate change. The study in turn stresses the significance of accounting for UHI loads in estimating urban energy use, for which a combined simulation approach of using an urban climate model and a building energy model has been presented as a feasible pathway to assess the impact of different urban constructions.

6 Appendix

Table 2. Key parameters used for simulations

	Parameter description	Moorgate based parameters
Block	Canyon and context block dimensions	L: 60 m × D: 35 m × H: 24.5 m
	Average floor height and storeys	3.5 m × Seven storeys
	Assumed building use and area in radius	Medium office; 3,410,400 m^2
Simplified Constructions ***Stone***	Wall material and thickness	Portland stone / gypsum plaster Thickness: 0.3 / 0.025 m; U-value: 2.33
	Roof material and thickness (flat roof)	Gravel / expanded polystyrene / concrete / ceiling tiles Thickness: 0.075 / 0.1 / 0.3 / 0.05 m; U-value: 0.24
	Glazing	GR: 0.3; U-value: 1.93 W m^{-2} K^{-1}
	Initial temperature of construction	20 ˚C
	Gains: lighting/equipment/occupancy	12 W m^{-2} / 25 W m^{-2} / 6 m^2 $person^{-1}$ Based on medium office schedules
	Infiltration and ventilation	0.5 ach and 0.002 m^3 s^{-1} m^{-2} respectively
	Cooling system and heating efficiency	Air and 0.80 respectively
	Daytime and night-time set points	Based on medium office schedule
	Heat rejected to canyon	50 %
Simplified Construction ***Glazed***	Wall material and thickness	Anti-sun glass cladding / expanded polystyrene / gypsum plasterboard Thickness: 0.010 / 0.1 / 0.025 m; U-value: 0.31
Roads	Material and Thickness	Asphalt / 0.5 m
Urban & rural road	Vegetation coverage ratio	0.005 and 0.8 respectively
Urban area	Average building height	24.5 m
	Horizontal building density ratio	0.598
	Vertical to horizontal urban area ratio	0.99
	Non-building sensible & latent heat rejection	22.68 W m^{-2} and 2.268 W m^{-2} respectively
	Characteristic neighbourhood radius	500 m
	Day and night-time UBL heights	1000 m and 80 m respectively
	Tree coverage ratio	0.001
	Tree and grass latent fractions	0.7 and 0.5 respectively
	Vegetation albedo	0.25
	Vegetation contribution start-end	4-10 (months)
Reference site ***Reading***	Latitude, longitude for Reading	51.446, - 0.957
	Distance from Moorgate site	~60 km due west

References

Bueno, B., Norford, L., Hidalgo, J. and Pigeon, G. (2013) 'The urban weather generator', *Journal of Building Performance Simulation,* 6(4), 269-281.

Bueno, B., Norford, L., Pigeon, G. and Britter, R. (2012) 'A resistance-capacitance network model for the analysis of the interactions between the energy performance of buildings and the urban climate', *Building and Environment,* 54, 116-125.

Bueno, B., Roth, M., Norford, L. and Li, R. (2014) 'Computationally efficient prediction of canopy level urban air temperature at the neighbourhood scale', *Urban Climate,* 9, 35-53.

Chandler, T. J. (1965) *The Climate of London,* London: Hutchinson & Co Ltd.

Doick, K. J., Peace, A. and Hutchings, T. R. (2014) 'The role of one large greenspace in mitigating London's nocturnal urban heat island', *Sci Total Environ,* 493, 662-71.

Eames, M., Kershaw, T. and Coley, D. (2011) 'On the creation of future probabilistic design weather years from UKCP09', *Building Services Engineering Research & Technology,* 32(2), 127-142.

Gartland, L. (2008) *Heat Islands: Understanding and Mitigating Heat in Urban Areas,* Oxford: Routledge.

Giridharan, R. and Kolokotroni, M. (2009) 'Urban heat island characteristics in London during winter', *Solar Energy,* 83(9), 1668-1682.

Grimmond, C., Roth, M., Oke, T. R., Au, Y., Best, M., Betts, R., Carmichael, G., Cleugh, H., Dabberdt, W. and Emmanuel, R. (2010) 'Climate and more sustainable cities: climate information for improved planning and management of cities (producers/capabilities perspective)', *Procedia Environmental Sciences,* 1, 247-274.

Howard, L. (1833) *The climate of London : deduced from meteorological observations made in the metropolis and at various places around it,* London: Harvey and Darton, J. and A. Arch, Longman, Hatchard, S. Highley [and] R. Hunter.

Iamarino, M., Beevers, S. and Grimmond, C. S. B. (2012) 'High-resolution (space, time) anthropogenic heat emissions: London 1970-2025', *International Journal of Climatology,* 32(11), 1754-1767.

IES-VE (2015) IES-Virtual Environment 2015, V 2015.1.0.0, Glasgow: Integrated Environmental Solutions Ltd.

Jacobson, M. Z. (2005) *Fundamentals of atmospheric modeling,* Cambridge: Cambridge University Press.

Kolokotroni, M. and Giridharan, R. (2008) 'Urban heat island intensity in London: An investigation of the impact of physical characteristics on changes in outdoor air temperature during summer', *Solar Energy,* 82(11), 986-998.

Masson, V. (2000) 'A physically-based scheme for the urban energy budget in atmospheric models', *Boundary-Layer Meteorology,* 94(3), 357-397.

Nakano, A., Bueno, B., Norford, L. and Reinhart, C. F. (2015) 'Urban Weather Generator - A novel workflow for integrating urban heat island effect within urban design process', in *Building Simulation 2015*, Hyderabad, India, International Building Performance Simulation Association,

Norford, L., Reinhart, C., Nakano, A., Bueno, B., Sullivan, J., Street, M., Zhang, L. and Lopez-Pineda, B. T. (2015) Urban Weather Generator, V 4.1.0, Cambridge, Massachusetts: Building Technology Program, Massachusetts Institute of Technology.

Norford, L., Reinhart, C., Nakano, A., Bueno, B., Sullivan, J., Street, M., Zhang, L., Lopez-Pineda, B. T., Yang, J. and Gunawardena, K. (2017) Urban Weather Generator, V 5.1.0 beta, Bath: University of Bath.

Oke, T. R. (1982) 'The Energetic Basis of the Urban Heat-Island', *Quarterly Journal of the Royal Meteorological Society,* 108(455), 1-24.

Oke, T. R. (1987) *Boundary Layer Climates,* 2 ed., New York: Routledge.

Taha, H. (1997) 'Urban climates and heat islands: Albedo, evapotranspiration, and anthropogenic heat', *Energy and Buildings,* 25(2), 99-103.

Taha, H., Akbari, H., Rosenfeld, A. and Huang, J. (1988) 'Residential Cooling Loads and the Urban Heat-Island - the Effects of Albedo', *Building and Environment,* 23(4), 271-283.

UN (2014) *World Urbanization Prospects: Highlights*, 2014 Revision, New York: United Nations.

Watkins, R., Palmer, J., Littlefair, P. and Kolokotroni, M. (2002) 'The London Heat Island: results from summertime monitoring', *Building Serv. Eng. Res. Technol.,* 23(2), 97-106.

Wilby, R. L. (2003) 'Past and projected trends in London's urban heat island', *Weather,* 58.